Figure S1

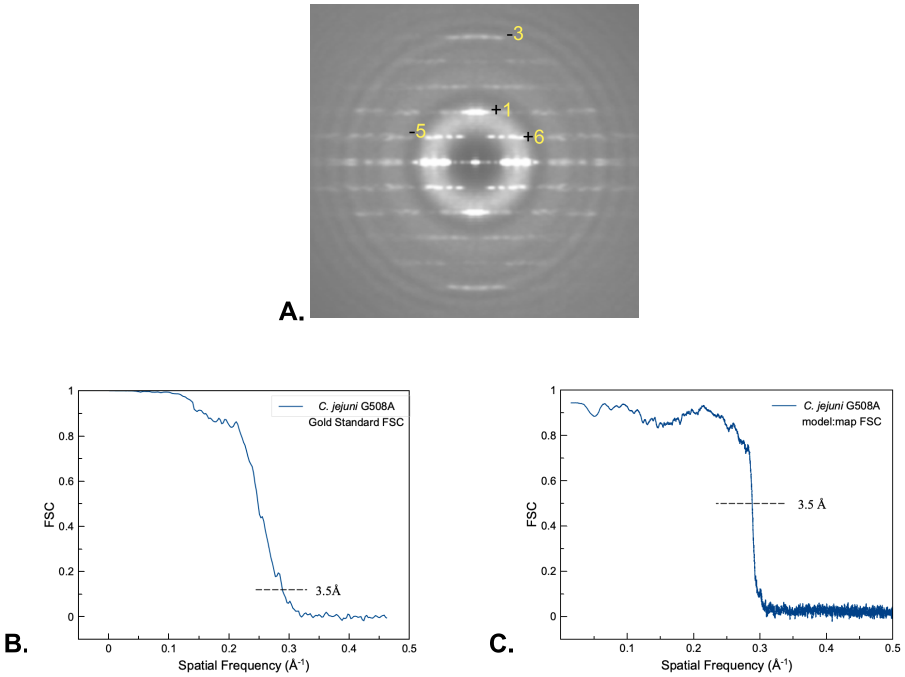

Figure S1. (A) The indexed power spectrum of the *C. jejuni* G508A flagellar filament. (B) FSC plot using the "gold-standard" map:map method. (C) FSC plot using the model:map method with a cutoff of 0.5.

www.pnas.org/cgi/doi/10.1073/pnas.2010996117

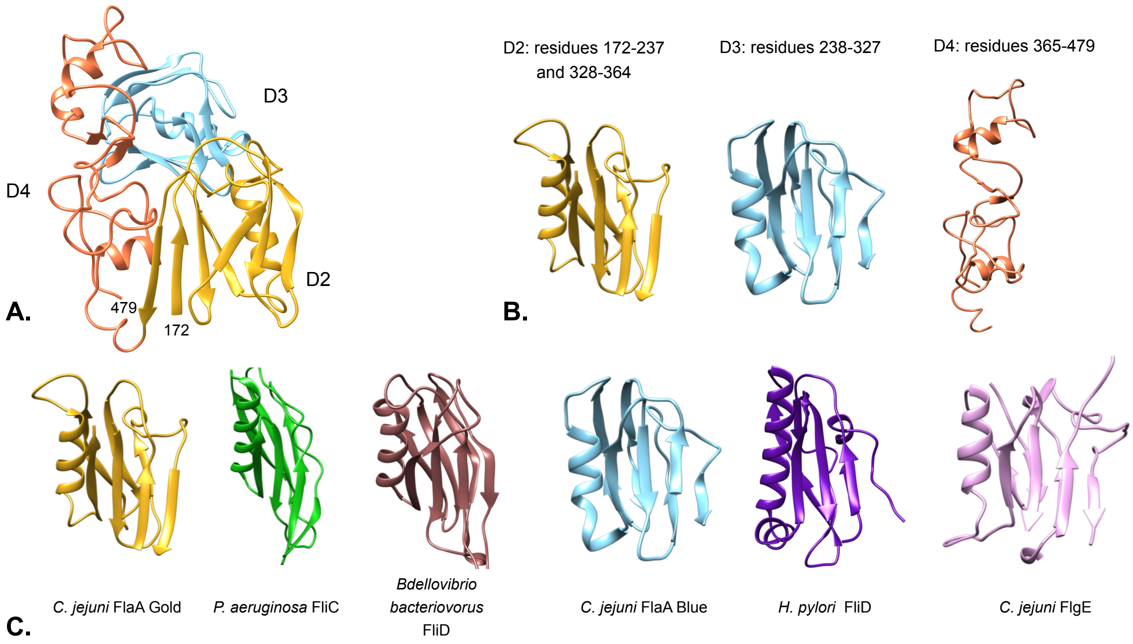

Figure S2

Figure S2. Domain duplication and structural homologs of the *C. jejuni* outer domain D2. (A) The outer domains D2 (gold), D3 (blue) and D4 (orange) of the *C. jejuni* flagellin). (B) The three outer domains shown separately. (C) Structural homology between the domain duplicated D2/D3 and domains from various flagella proteins.

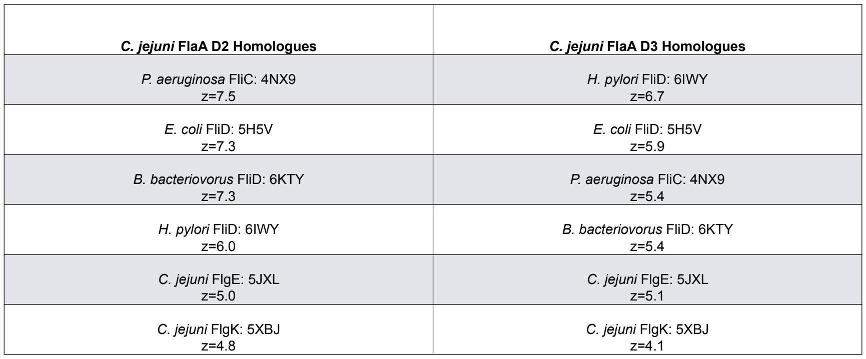

***C. jejuni* FlaA D2 Homologues**	***C. jejuni* FlaA D3 Homologues**
P. aeruginosa FliC: 4NX9 z=7.5	*H. pylori* FliD: 6IWY z=6.7
E. coli FliD: 5H5V z=7.3	*E. coli* FliD: 5H5V z=5.9
B. bacteriovorus FliD: 6KTY z=7.3	*P. aeruginosa* FliC: 4NX9 z=5.4
H. pylori FliD: 6IWY z=6.0	*B. bacteriovorus* FliD: 6KTY z=5.4
C. jejuni FlgE: 5JXL z=5.0	*C. jejuni* FlgE: 5JXL z=5.1
C. jejuni FlgK: 5XBJ z=4.8	*C. jejuni* FlgK: 5XBJ z=4.1

Table S1

Table S1: Structural homologs of *C. jejuni* FlaA D2 and D3.

Amino Acid residue
S343
S348
T394
S398
S401
S405
S412
S418
S426
S430
S437
S441
S443
S449
S455 *
S461*
T469

A.

1 MGFRINTNVAALNAKANSDLNAKSLDASLSRLSSGLRINSAAD 43

44 DASGMAIADSLRSQANTLGQAISNGNDALGILQTADKAMDEQL 86

87 KILDTIKTKATQAAQDGQSLKTRTMLQADINKLMEELDNIANT 129

130 TSFNGKQLLSGNFTNQEFQIGASSNQTVKATIGATQSSKIGVT 172

173 RFETGAQSFTSGVVGLTIKNYNGIEDFKFDNVVISTSVGTGLG 215

216 ALAEEINKSADKTGVRATYDVKTTGVYAIKEGTTSQEFAINGV 258

259 TIGKIEYKDGDGNGSLISAINAVKDTTGVQASKDENGKLVLTS 301

302 ADGRGIKITGDIGVGSGILANQKENYGRLSLVKNDGRDINISG 344

345 TNLSAIGMGTTDMISQSSVSLRESKGQISATNADAMGFNSYKG 387

388 GGKFVFTQNVSSISAFMSAQGSGFSRGSGFSVGSGKNLSVGLS 430

431 QGIQIISSAASMSNTYVVSAGSGFSSGSGNSQFAALKTTAANT 473

474 TDETAGVTTLKGAMAVMDIAETAITNLDQIRADIGSIQNQVTS 516

517 TINNITVTQVNVKAAESQIRDVDFASESANYSKANILAQSGSY 559

560 AMAQANSSQQNVLRLLQ 576

B.

Figure S3

Figure S3: Glycosylation sites detected in the *C. jejuni* FlaA Flagellin. (A) List of glycosylated residues seen in the *C. jejuni* FlaA density map. (B) FlaA sequence showing each of the observed glycosylated residues in red

Fig S4

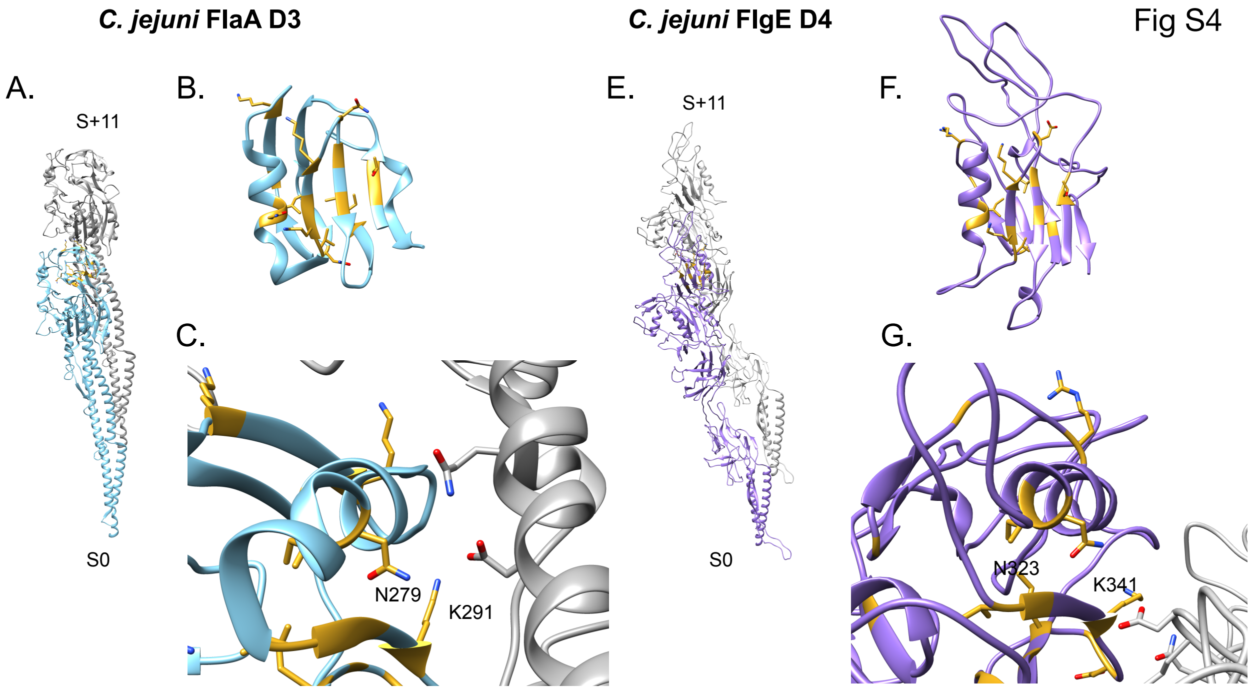
***C. jejuni* FlaA D3**

***C. jejuni* FlgE D4**

Figure S4: Comparison of *C. jejuni* FlaA D3 (A-C) and FlgE D4 (D-F) along their 11-start interfaces. (A) Two flagellins along the same protofilament are shown. (B) Residues that are conserved or similar in *C. jejuni* FlaA to *C. jejuni* FlgE are colored in gold. (C) A close up of the FlaA D3 11-start interface shows two key conserved residues (N279 and K291) between FlaA and FlgE. (D-F) As with A-C, two flagellar hook proteins along the same protofilament are shown. (E) Residues that are conserved or similar in *C. jejuni* FlgE to *C. jejuni* FlaA are colored in gold. (F) Two conserved residues along the 11-start interface in FlgE domain D4 are N323 and K341.

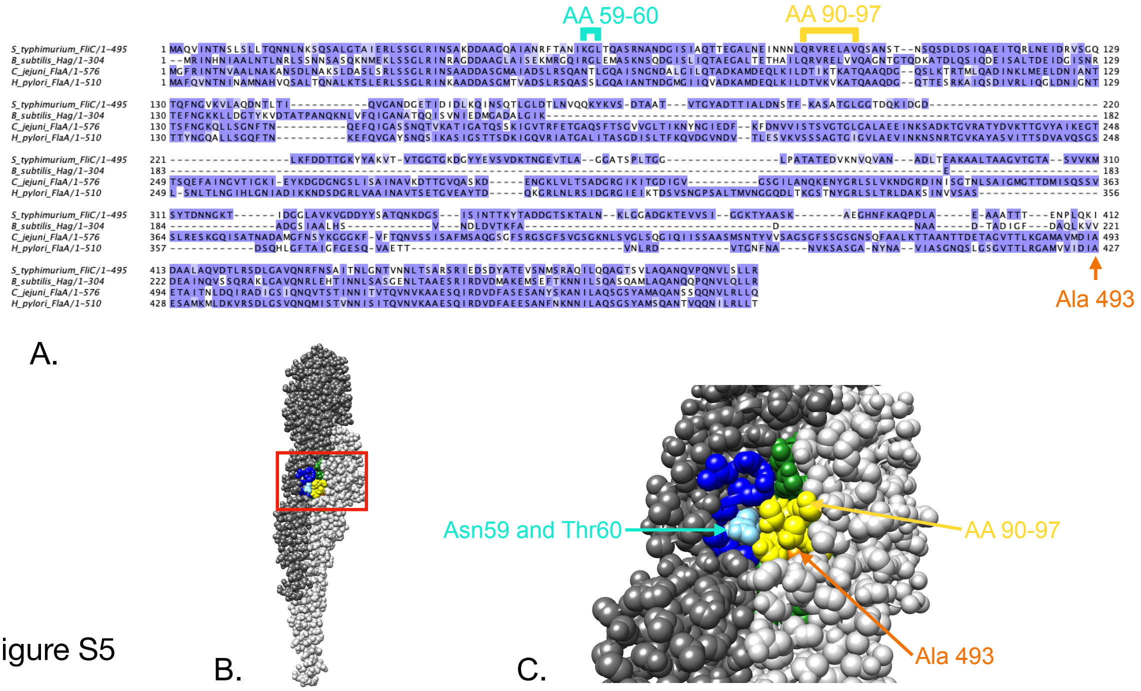

Figure S5

Figure S5: Sequence changes in the residues interfacing the TLR5 epitope previously suggested to allow for motility in *H. pylori and C. jejuni*. (A) Multiple sequence alignment of several key bacterial flagellins. (B) Space filling representation of two flagellins along the 11-start protofilament. The S0 flagellin is shown in light gray while the S+11 is in dark grey. (C) A close up of the interface site between the two flagellins confirming the previously reported predictions about the *H. pylori* and *C. jejuni* flagellins.

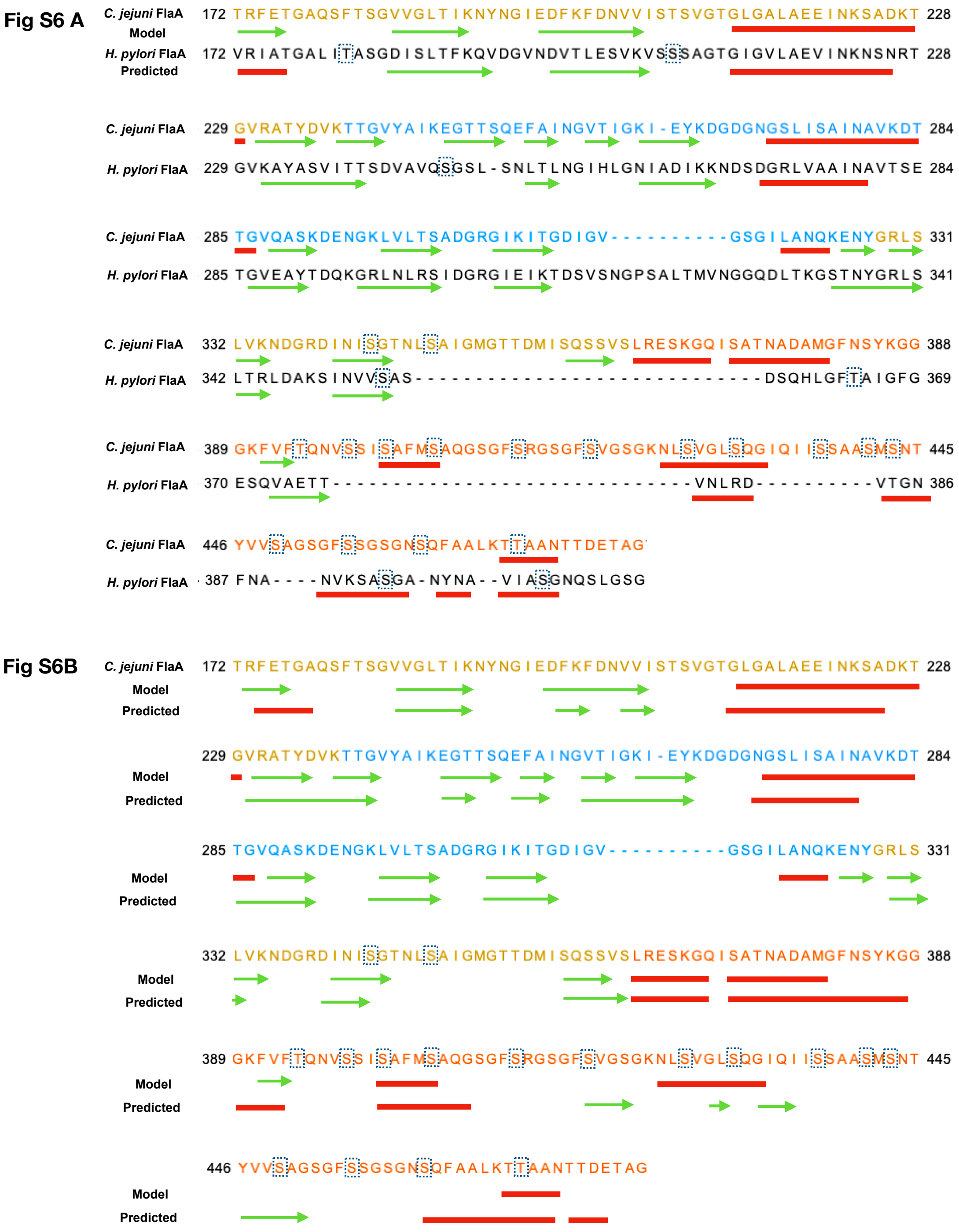

Figure S6: Sequence alignment and secondary structure of the *C. jejuni* and *H. pylori* FlaA flagellins. (A) Sequence alignment showing the observed secondary structure in *C. jejuni* FlaA and the predicted *H. pylori* FlaA secondary structure. (B) A comparison between the observed and predicted secondary structure of *C. jejuni* G508A.